



2 A proposed working standard for the measurement of diffuse 3 horizontal shortwave irradiance

4 J. J. Michalsky,¹ C. Gueymard,² P. Kiedron,³ L. J. B. McArthur,⁴ R. Philipona,⁵
5 and T. Stoffel⁶

6 Received 12 March 2007; revised 8 June 2007; accepted 19 June 2007; published XX Month 2007.

7 [1] Atmospheric radiative transfer model estimates of diffuse horizontal broadband
8 shortwave (solar) irradiance have historically been larger than measurements from a
9 shaded pyranometer. A reference standard for the diffuse horizontal shortwave irradiance
10 does not exist. There are no current efforts to develop an absolute standard that are
11 known to the authors. This paper presents the case for a working standard for
12 this measurement. Four well-behaved pyranometers from two previous intensive
13 observation periods (IOP) were chosen for this study. The instruments were characterized
14 for spectral and angular response before the IOP and calibrated during the IOP using a
15 shade/unshade technique with reference direct irradiance from an absolute cavity
16 radiometer. The results of the comparison and detailed analyses to explain the differences
17 suggest selecting three of the four for the working standard. The 95% confidence
18 uncertainty in this standard is estimated at 2.2% of reading + 0.2 W/m². In lieu of a
19 comparison to this trio, a procedure for obtaining low-uncertainty diffuse horizontal
20 shortwave irradiance is suggested.

21 **Citation:** Michalsky, J. J., C. Gueymard, P. Kiedron, L. J. B. McArthur, R. Philipona, and T. Stoffel (2007), A proposed working
22 standard for the measurement of diffuse horizontal shortwave irradiance, *J. Geophys. Res.*, *112*, XXXXXX,
23 doi:10.1029/2007JD008651.

25 1. Introduction

26 [2] The motivation for improving the measurement of
27 diffuse horizontal broadband shortwave irradiance (hereaf-
28 ter, diffuse or diffuse irradiance) was discussed thoroughly
29 by *Michalsky et al.* [2003], which describes the first diffuse
30 intensive observation period (IOP), and in *Michalsky et al.*
31 [2005], which describes the second diffuse IOP; conse-
32 quently, the motivation for this effort will be brief. Clear-
33 sky radiative transfer models of diffuse irradiance are
34 persistently higher than measurements, especially for mod-
35 est aerosol loads. Recently, *Michalsky et al.* [2006] com-
36 pared six radiative transfer models with clear-sky
37 measurements for a wide range of aerosol loads and solar
38 angles. This study demonstrated that better diffuse measure-
39 ments with a better specification of the surface albedo and
40 better aerosol optical property specifications, especially
41 asymmetry parameter, narrowed the average bias to under
42 2% or about 2 W/m² for the 30 cases investigated.

[3] The purpose of this third diffuse IOP, conducted 43
between 10 and 19 October 2006, was to select from among 44
the best pyranometers in the first and second diffuse IOPs. 45
Elimination of pyranometers to be included in the standard 46
is based on one or more of the following: noisy signals, 47
instability with respect to the other instruments within the 48
overall group, and poor offset corrections. The pyranome- 49
ters chosen for the standard were characterized for individ- 50
ual spectral and angular responses in order to explain any 51
discrepancies that might arise during the comparisons. The 52
goal was to develop a reliable, diffuse-irradiance working 53
standard that will minimize the likelihood that the discrep- 54
ancy with models can be attributed to diffuse measurement 55
uncertainty. 56

[4] In the next section the instrumentation is highlighted 57
including a discussion of the calibration of the pyranometers 58
and the thermal offset (zero) corrections. Section 3 illus- 59
trates the results from a few days that indicate cloudy-sky 60
and clear-sky behavior of the group of pyranometers before 61
recalibration and offset correction and after these correc- 62
tions are applied. Section 4 describes the characterization of 63
the pyranometers for spectral response including reflectivity 64
of the receiver surfaces. Calculations are presented that 65
model how the spectral character of the instruments could 66
cause differences in response. The angular responses of the 67
pyranometers are shown, with some results regarding the 68
changes that could arise because of angular response differ- 69
ences under cloudy and clear skies. Completely independent 70
methods to measure diffuse that can be used to decide 71
among dissident measurements are described in section 5. 72

¹Earth System Research Laboratory, NOAA, Boulder, Colorado, USA.

²Solar Consulting Services, Colebrook, New Hampshire, USA.

³Cooperative Institute for Research in Environmental Sciences, University of Colorado, Boulder, Colorado, USA.

⁴Meteorological Service of Canada, Downsview, Ontario, Canada.

⁵Physikalisch-Meteorologisches Observatorium Davos and World Radiation Center, Davos, Switzerland.

⁶National Renewable Energy Laboratory, Golden, Colorado, USA.

t1.1 **Table 1.** Pyranometers Used for the IOP, Response Measurements, Standard Deviation of New Responses, and Offsets

t1.2 Instrument	Serial Number	Response (Old), $\mu\text{V}/\text{W}/\text{m}^2$	Response (New), $\mu\text{V}/\text{W}/\text{m}^2$	Standard Deviation of 30-Point Sample	Predicted Offset, W/m^2	Capped Offset, W/m^2
t1.3 cm22rp ^a	990010	11.46	11.46 $\mu\text{V}/\text{W}/\text{m}^2$	0.03 $\mu\text{V}/\text{W}/\text{m}^2$	-0.7	-0.9
t1.4 cm22 ^b	010047	9.6027	9.76	0.03	-1.6	-1.2
t1.5 cm11 ^c	069059	8.43	8.31	0.02	-2.5	-2.3
t1.6 8-48 ^d	34580	9.62	9.66	0.03	+0.1	+0.7

t1.7 ^aKipp & Zonen, Inc. CM 22; provided by Rolf Philipona with a custom VHS ventilator with heating.t1.8 ^bKipp & Zonen, Inc. CM 22; Kipp & Zonen CV2 ventilator with no heating.t1.9 ^cKipp & Zonen, Inc. CM 11B; Kipp & Zonen CV2 ventilator with no heating.t1.10 ^dEppley Laboratory, Inc. 8-48; Eppley Laboratory, Inc. VEN ventilator with no heating.

73 Section 6 summarizes these discussions. Section 7 suggests
 74 a triad of pyranometers as a diffuse working standard with
 75 their estimated uncertainty. A method to use for diffuse
 76 measurements if a comparison to this triad is not possible is
 77 suggested.

78 2. Pyranometers, Calibrations, and Offset 79 Corrections

80 [5] In this third diffuse IOP four pyranometers were used
 81 to measure diffuse irradiance simultaneously, and a pyrge-
 82 ometer was used to measure the net infrared for use in
 83 correcting the offsets of the pyranometers. Table 1 contains
 84 four well-behaved instruments from the second IOP
 85 [Michalsky *et al.*, 2005] that are used for this study. The
 86 third column contains the responses supplied by the owner
 87 or manufacturer of the pyranometer. The fourth and fifth
 88 columns contain the responses and standard deviations
 89 obtained from a shade/unshade calibration during the IOP
 90 that will be discussed below. The sixth column contains the
 91 predicted offsets, which will be discussed below, for the time
 92 the day when conditions are expected to produce the highest
 93 offsets, followed in column seven by the results of a
 94 capping experiment to measure the offsets.

95 [6] A shade/unshade calibration was performed for all
 96 four pyranometers centered near solar noon on 11 October
 97 2006 and then again on 13 October 2006 for the 8–48 only.
 98 The IOP dates were selected anticipating this calibration
 99 since the preferred solar angle for calibrating is 45° and the
 100 Sun remains within $\pm 1^\circ$ of this angle for about two hours
 101 around solar noon at the Department of Energy’s Atmo-
 102 spheric Radiation Measurement (ARM) Climate Research
 103 Facility’s (ACRF) Southern Great Plains (SGP) central site
 104 (36.607°N, 97.496°W). The four pyranometers were
 105 mounted on a tracker, thus maintaining their same orienta-
 106 tion in azimuth relative to the Sun. The level of the instru-
 107 ments was checked before the calibration. All pyranometers
 108 are alternately shaded and unshaded manually in the same
 109 order within 10–15 s and left in that condition for the
 110 remaining 2 or 3 min (see below) to permit the instrument to
 111 stabilize at its full-shade or full-Sun value. Since instru-
 112 ments have different time constants this stabilization time
 113 varies. In Figure 1a the shade and unshade periods were 3 min
 114 long, and a stable value was slowly approached because of
 115 the rather long time constant of the 8–48 pyranometer. Each
 116 dot is a 10-s average of 1-s samples. In Figure 1b the shade
 117 or unshade period is 2 min for the cm11 pyranometer and
 118 the instrument quickly settles to a stable value, as was true

for all of the Kipp and Zonen instruments. The ratio of the
 difference in voltage readings ($V_{unshade} - V_{shade}$) to the
 product of the direct irradiance, measured with an absolute
 cavity radiometer, and the cosine of the solar-zenith angle,
 sza , is the responsivity of the pyranometer:

$$\text{Response} = \frac{(V_{unshade} - V_{shade})}{\text{Direct Irradiance} \cdot \cos(sza)} \quad (1)$$

[7] Comparing columns three and four in Table 1, the
 calibration of the CM 22 from the World Radiation Center
 (cm22rp) had not changed from the shade/unshade calibra-
 tion performed during the second diffuse IOP [Michalsky *et al.*, 2005]. The other cm22 shade/unshade calibration
 yielded a 1.6% higher response than the calibration provided
 by the National Renewable Energy Laboratory (NREL),
 which did not use a shade/unshade technique for their
 calibration. The change in response for the cm11 was
 1.4% lower than the indoor calibration provided by the
 manufacturer. The 8–48 response was 0.4% higher than the
 manufacturer’s indoor calibration.

[8] The thermal offset correction used nighttime pyran-
 ometer measurements as a function of the net infrared (net-
 IR) signal from a colocated pyrgeometer. This technique for
 correcting offsets in pyranometers was explained by Dutton
et al. [2001]. Figure 2 illustrates this process for the cm11,
 which has the largest offset of the four pyranometers. Using
 only nighttime data with the Sun below the horizon (more
 than 7° below), the pyranometer reading is plotted versus
 the net-IR reading for nine nights of 10-s data, or over
 36,800 points. Each dot in Figure 2 is a 10-s average of 1-s
 samples. The linear least squares fit to all the data in Figure 2
 is the black line. The green (dashed) line is a robust fit to the
 data, which de-emphasizes outliers. The source of the out-
 liers that occurred during the IOP is uncertain, but they are
 associated with a disruption of the thermal balance of the
 pyranometers. The green (dashed) line is used to predict the
 offset for all conditions, both night and day. A stringent test
 of the offset correction is to estimate offsets in the early
 afternoon on a clear day. This produces a large, negative,
 net-IR irradiance (approximately $-150 \text{ W}/\text{m}^2$), outside the
 bounds of the nighttime signals. Higher net-IR irradiance
 occurs during the day than at night because the direct Sun
 heats the body of the pyranometer, which does not occur at
 night, while the dome that is blocked from direct sunlight
 radiates to space leading to an exacerbated difference in
 dome and case temperatures, thus causing a high net-IR

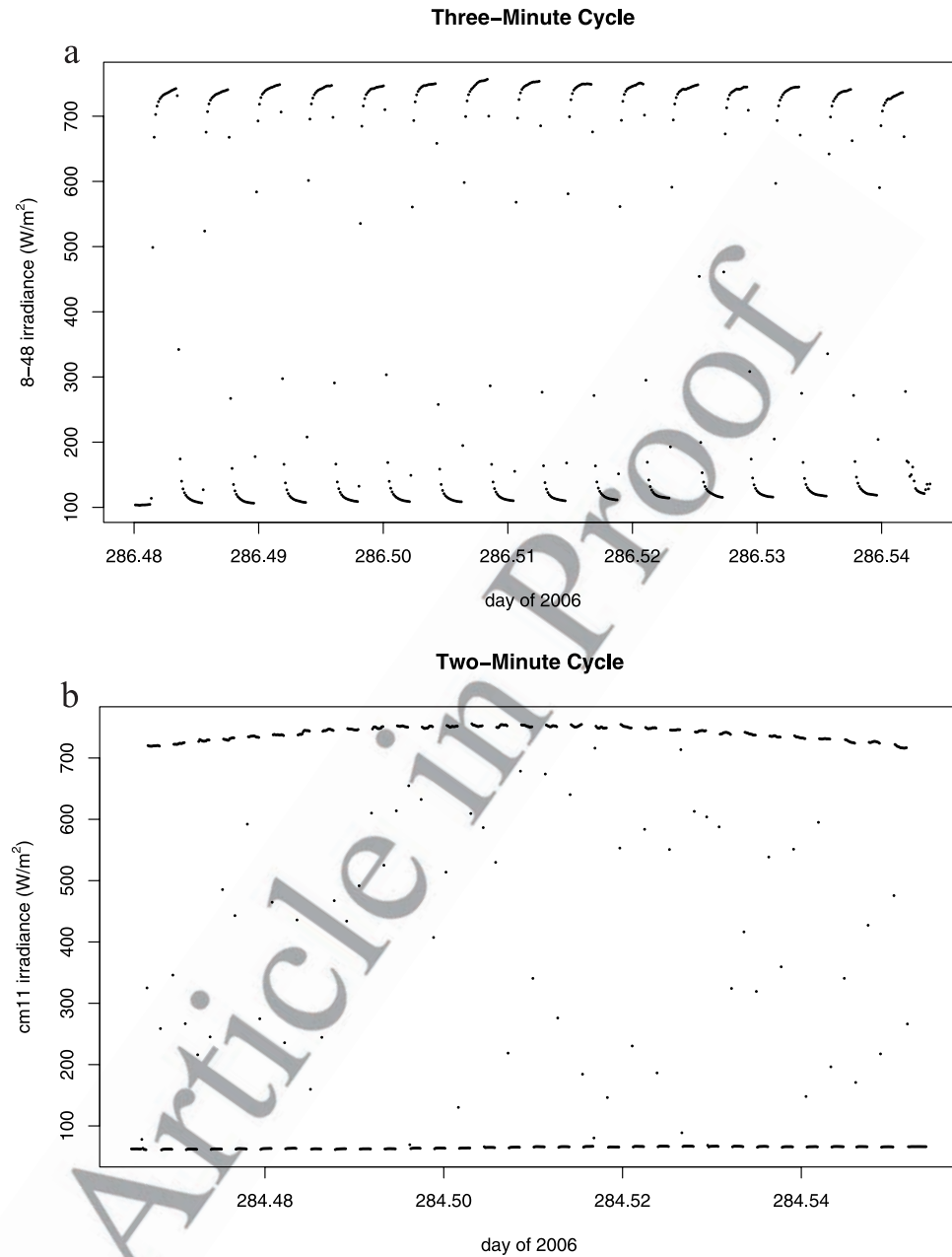


Figure 1. (a) For a shade-unshade calibration the 8–48 pyranometer is alternately shaded and unshaded (3 min each) and the difference is compared to the direct beam irradiance measured with an absolute cavity radiometer and multiplied by the cosine of the solar-zenith angle. (b) The same sequence of shading and unshading is repeated for the cm11 pyranometer with a 2_min cycle. Note the difference of the time responses of the two instruments; the $1/e$ 8–48 time response (5 s) is three times that of the cm11 (1.66 s).

164 signal. To assess the offset, the instrument dome is capped
 165 to block all incoming solar radiation. The best assessment of
 166 the offset occurs when the time constant of the detector is
 167 1–2 s, or shorter, so that the dome temperature experiences
 168 a minimal change because of the heat-trapping cap. As may
 169 be expected from Figure 1a, the 8–48 with its slow time
 170 constant may not satisfy this criterion, while the others
 171 respond very quickly to the blocked radiation and yield a
 172 reasonable estimate of the daytime offset. The last two

columns of Table 1 indicate that the predicted and measured
 173 offsets are within 0.4 W/m^2 except for the 8–48, as
 174 expected since the 8–48's slow response does not permit
 175 a true offset determination by this method. 176

[9] Using nighttime data to correct daytime measure-
 177 ments cannot account for the fact that during the daytime
 178 solar radiation heats the detector. The difference between
 179 the dome and detector temperatures causes the offset, and
 180 the proxy method to estimate the offset using the net-IR
 181

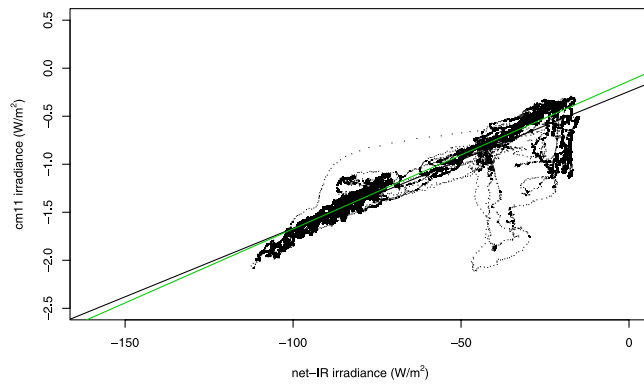


Figure 2. The offset prediction is determined by regressing offset at night versus the simultaneous thermopile net-IR from a colocated pyrgeometer. The outliers are caused by thermal imbalances associated with rainfall on the instruments. The black line is a linear least squares fit and the green (dashed) line is a robust fit that deweights outliers.

182 irradiance, which emulates the difference in dome and
 183 receiver temperature difference, may not hold if the detector
 184 is irradiated. One way to test whether the offset estimate
 185 based on the robust fit to the nighttime data is correct is to
 186 ratio the 8–48, an instrument which has almost no thermal
 187 offset, to the offset-corrected instruments, and then to plot
 188 this ratio as a function of incoming diffuse radiation. If the
 189 offset correction is inadequate, this ratio should increase
 190 with higher irradiance as the temperature difference between
 191 the dome and detector exceeds that estimated by the proxy
 192 measurement provided by the net-IR irradiance. Figure 3 is
 193 a plot of the ratio of the 8–48 to each of the three offset-
 194 corrected pyranometers as a function of diffuse irradiance.
 195 The data are screened to allow only diffuse irradiances that
 196 exceed 50 W/m^2 and for overcast conditions; the last
 197 requirement is to avoid confusing this effect with the clear
 198 versus cloudy sky effects that will be discussed in a later
 199 section. There is no significant increase in the ratio with
 200 irradiance. Although it increases slightly at low irradiances,
 201 the ratio is smaller at the highest irradiances. The 8–48/
 202 cm11 ratio has the largest change in the top of Figure 3, but
 203 the maximum effect is only slightly larger than 1% suggest-
 204 ing that the offset correction scheme is adequate. Since we
 205 have chosen cloudy conditions for this plot, the dome and
 206 case difference caused by cooling to space is small in the
 207 pyrgeometer, but if the detector heating in the pyranometer
 208 causes a detector-dome temperature difference in this in-
 209 strument, then the effect of inadequate offset corrections
 210 should be detected in these plots, but is not.

211 [10] Note that the ratios in Figure 3 are consistently
 212 greater than one: this suggests that the 8–48 irradiances
 213 are too high relative to the other instruments. This could be
 214 the result of what Figure 1a illustrates. The shaded and
 215 unshaded values do not quite arrive at asymptotic values
 216 suggesting that the numerator of equation (1) should be
 217 larger. A larger response would result in a smaller cali-
 218 bration constant (the inverse of the response) and, therefore,
 219 lower irradiances.

[11] As in the second IOP [Michalsky *et al.*, 2005], the
 shading and receiver geometry is the same for all pyran-
 ometers, thus eliminating different receiver views of the
 solar aureole as a source of differences.

3. Comparisons of the Diffuse Irradiances

[12] Figure 4 contains three plots. The pyranometers and
 the pyrgeometer were mounted on trackers that provided
 shading for the instruments all day. The top plot is the
 diffuse irradiance from each of the four pyranometers. In
 this plot the offsets are not corrected and the original
 calibrations from Table 1, column 3 are used. In the middle
 plot the offsets are corrected and the shade-unshade cali-
 brations from Table 1, column 4, are applied. The 8–48 has
 an additional multiplicative factor of 0.98 applied to the data
 to correct for the underestimate of responsivity as discussed
 in the last section. This correction was based on forced
 agreement with the other three instruments when totally
 overcast conditions prevailed. In the bottom plot the ratio of
 each corrected output to the corrected output of pyranom-
 eter cm22rp is plotted. The diffuse signal is also plotted with
 the values in W/m^2 labeled on the right-hand side. This day

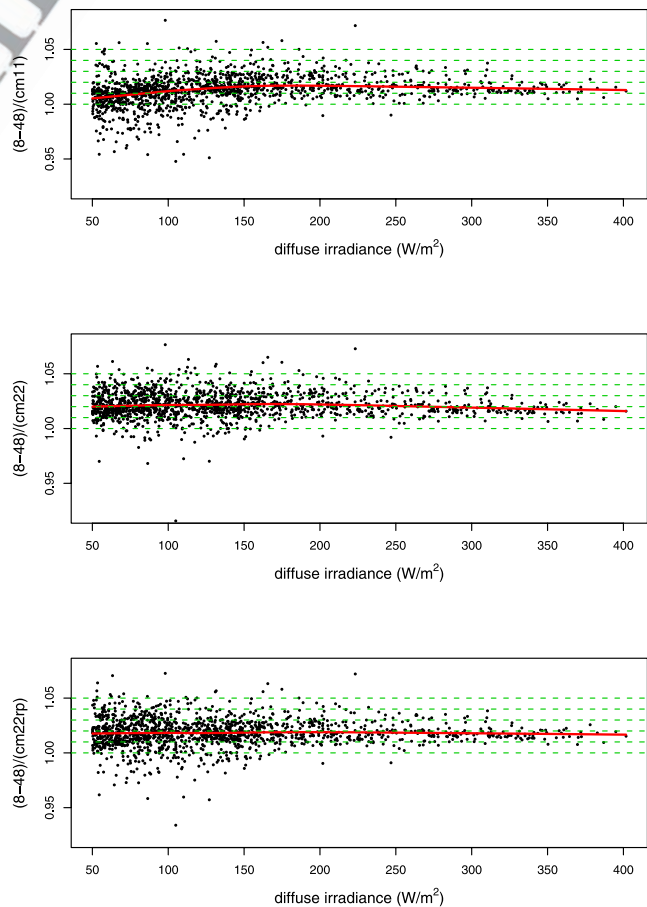


Figure 3. These are plots of the ratio of the 8–48 to each of the Kipp and Zonen pyranometers as a function of the cloudy-sky irradiance. Points are screened to select overcast skies with diffuse exceeding 50 W/m^2 . There is no obvious dependence of the offset correction on the heating of the sensor by solar flux.

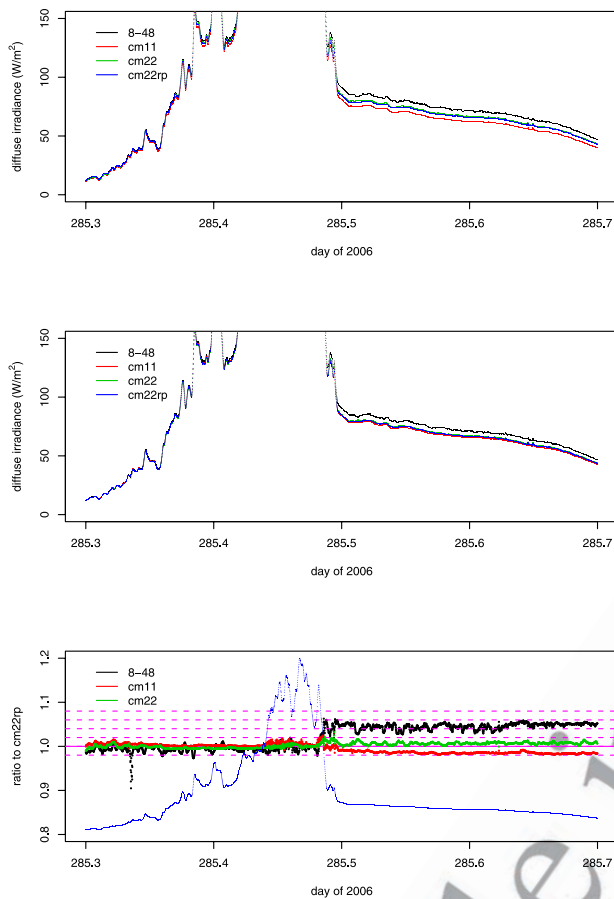


Figure 4. (top) Diffuse irradiance for the four instruments with original calibrations and no offset corrections for a day that was overcast in the morning and completely clear in the afternoon. (middle) The data are offset corrected and the shade-unshade calibrations applied. The 8_48 has an additional adjustment of 2% as discussed in the text. (bottom) A ratio of each pyranometer to the cm22rp.

241 was completely overcast in the morning, and completely
 242 clear after solar noon with a rapid transition between these
 243 two conditions. The difference between the top and middle
 244 plots indicates slightly improved agreement in the morning
 245 among all pyranometers (the overplot looks like a single
 246 instrument). In the afternoon the cmxx pyranometers of
 247 Kipp and Zonen indicate modest separation, but the 8–48
 248 reads notably higher relative to these. The bottom plot
 249 clearly shows the abrupt change in the ratio of the 8–48
 250 to cm22rp associated with clearing skies.

251 [13] Figure 5 is similar to Figure 4, but the sky is covered
 252 by cirrus during most of this day. The bottom plot's right-
 253 hand axis is direct normal irradiance. This plot shows that
 254 the direct beam passes through transparent cirrus clouds
 255 whose thicknesses are insufficient to completely extinguish
 256 the solar beam. The 8–48 irradiance is higher throughout the
 257 day, but the ratio to the cm22rp is smaller than it was in
 258 the clear portion of Figure 4. An examination of all similar
 259 plots for the IOP reveals that clear skies produce ratios of
 260 the 8–48 to the cm22rp that are in the range of 1.04 to 1.05
 261 for the clearest skies, about 1.00 for the cloudiest, with

intermediate values for conditions such as in Figure 5. 262
 Attempts to explain these differences follow. 263

4. Spectral and Angular Response Differences 264

[14] The agreement among all four pyranometers when 265
 there is complete overcast is near 1% for irradiances above 266
 50 W/m^2 to ensure that the instrumental signal-to-noise ratio 267
 is not an issue. For clear conditions the three Kipp and 268
 Zonen instruments (designated collectively as cmxx) agree 269
 within 2% even though there are differences in how the 270
 instruments are constructed (different dome glasses) or 271
 operated (different ventilation). The 8–48 disagreement is 272
 highest for clear conditions and somewhat less for cirrus- 273
 covered skies. 274

[15] An obvious difference, as suggested by Michalsky *et* 275
al. [2005] for the second diffuse IOP, is the spectral 276
 distribution of scattered radiation from these different skies 277
 [e.g., see Michalsky *et al.*, 2005, Figure 10]. The cloudy sky 278
 has a spectral distribution similar to the Sun, but the clear- 279
 sky distribution is shifted well to the blue relative to the 280
 solar spectrum because of the predominance of Rayleigh 281
 scattering. It is possible to model the relative responses of 282

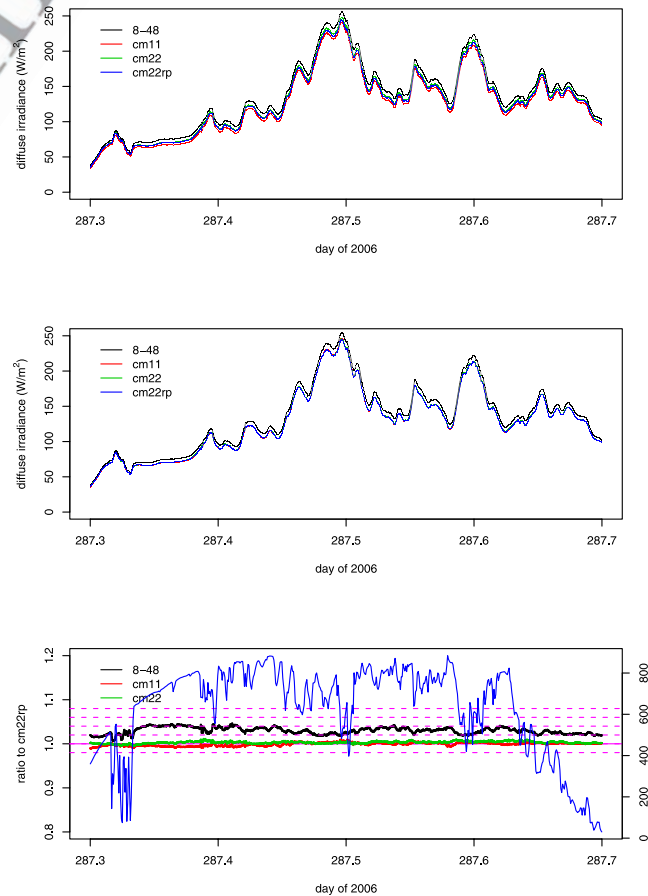


Figure 5. The same plot sequence as in Figure 4 is shown except the bottom plot's right-hand side is direct irradiance rather than diffuse. This direct beam plot indicates when cirrus clouds are present and demonstrates that cirrus produces a smaller 8–48 to cm22rp ratio than in Figure 4, which depends on the extent of the cirrus cover.

t2.1 **Table 2.** Difference in Clear-Sky Diffuse Irradiance Responses if Calibrated by Shade-Unshade

t2.2	Pyranometer	Dome Glass (T)	Sensor Absorber (A)	$I_{\text{diffuse-measured}}/I_{\text{diffuse-model}}$
t2.3	Eppley 8–48	Schott WG295	NRC-measured white	1.011
t2.4			NRC-measured black	
t2.5	Kipp&Zonen CM11	Schott N-K5	Kipp&Zonen data	0.988
t2.6	Kipp&Zonen CM22	Tydex KS-4V(quartz)	Kipp&Zonen data	0.996

283 the different instruments if we have the transmissions of the
 284 glasses, the spectral absorptions of the receivers, and the
 285 spectral distribution of the incident irradiances. In the work
 286 by *Michalsky et al.* [2005], generic absorptions and trans-
 287 missions were used to posit a plausible explanation for why
 288 the instruments disagree. In preparation for this IOP, spec-
 289 tral measurements of the reflection from coupons, which are
 290 similar to the receiver surfaces in a new Eppley 8–48 black
 291 and white pyranometer, were made by the National
 292 Research Council of Canada from 250 to 2200 nm. The
 293 Kipp and Zonen pyranometers all use the same black paint
 294 for their receivers. Kipp and Zonen provided the spectral
 295 absorption for their receivers. Both manufacturers also
 296 provided transmission curves for the types of glasses used.
 297 We used the SMARTS model [*Gueymard*, 2001] to produce
 298 plausible spectra for conditions during the IOP.

299 [16] As discussed by *Michalsky et al.* [2005] the signal
 300 from a single black thermopile detector instrument depends
 301 on the absorption of the paint A , the transmission through
 302 the dome or domes T , and the spectral distribution of the
 303 incoming solar radiation I , all as a function of wavelength λ .
 304 A pseudo-calibration of the instruments is performed using
 305 modeled direct solar radiation on a horizontal surface as in
 306 our shade-unshade field calibration. Therefore the pyran-
 307 ometer “signal” is represented as follows

$$S_{\text{direct-horizantal}} = K \cdot \int_{\lambda} I_{\text{direct-horizantal}}(\lambda) A(\lambda) T(\lambda) d\lambda. \quad (2)$$

310 [17] The irradiance received from the direct beam falling
 311 on the horizontal is $\int I_{\text{direct-horizantal}}(\lambda) d\lambda$. The pseudo-
 312 calibration of the pyranometer is this last term divided by
 313 equation (2), or

$$\frac{\int_{\lambda} I_{\text{direct-horizantal}}(\lambda) d\lambda}{K \cdot \int_{\lambda} I_{\text{direct-horizantal}}(\lambda) A(\lambda) T(\lambda) d\lambda}. \quad (3)$$

316 [18] The pyranometer “signal” from the diffuse irradi-
 317 ance is similar to equation (2)

$$S_{\text{diffuse}} = K \cdot \int_{\lambda} I_{\text{diffuse}}(\lambda) A(\lambda) T(\lambda) d\lambda. \quad (4)$$

320 [19] The product of equations (3) and (4) produces the
 321 pseudo-diffuse irradiance that would be measured by a
 322 pyranometer calibrated with the shade-unshade method.
 323 The constant of proportionality K in equations (3) and
 324 (4) cancels. This irradiance can then be compared with
 325 $\int_{\lambda} I_{\text{diffuse}}(\lambda) d\lambda$.

[20] For the case of an 8–48 we substitute the difference
 in black and white surface absorption for the single black
 surface absorption. Table 2 contains the ratios of the
 pyranometer “diffuse measurements” (products of equa-
 tions (3) and (4)) to the diffuse obtained by integration of
 the modeled clear-sky diffuse irradiances.

[21] The Kipp and Zonen cm22 has the closest response
 to the modeled irradiance, but is low by about 0.4%. The 8–
 48 is high by about 1.1% and the cm11 is low by about
 1.2%. Consequently, the 8–48 for clear skies should read
 about 1.5% high relative to the cm22. The spectral effect is,
 therefore, in the direction indicated in Figures 4 and 5, but
 the difference is about a third of the difference that needs to
 be explained. The bottom of Figure 4 indicates that the
 cm11 shifts from agreeing with the cm22rp during the
 cloudy part of the day to reading low relative to the cm22rp
 during the clear afternoon, which is the observed direction
 and roughly the magnitude of the shift expected from Table 2
 if all of the shift is caused by spectral response.

[22] A further difference between clear skies and overcast
 skies is the spatial distribution of the diffuse radiation. This
 was also discussed in the second IOP paper [*Michalsky et al.*,
 2005]. In that paper plausible arguments were made for
 why the 8–48 could measure higher relative to other
 instruments in a clear versus cloudy sky. Generic angular
 responses were used to calculate the differences. For this
 study the angular responses of the four pyranometers were
 measured in four cardinal directions at the National Atmo-
 spheric Radiation Centre (Canada). The results of those
 measurements for the four instruments in the IOP are
 plotted in Figure 6. The 8–48 has a super cosine response
 in three of the directions plotted, i.e., as the elevation angle
 gets lower the response is higher than a true cosine response
 for three directions. The cm11 has a tendency to fall off
 slightly and then rise to be nearer to true cosine at the largest
 angle measured. The cm22 and cm22rp behave similarly for
 the most part. All instruments have what generally would be
 considered good angular responses, deviating less than 5%
 from true cosine, except at the largest angle measured of
 80°.

[23] To estimate the effects of cosine response on the
 level of agreement among measurements, two models of
 skylight distribution were used. Although these are distri-
 butions for luminance, they are approximately correct for
 radiance. The *Moon and Spencer* [1942] model was adopted
 for cloudy-sky calculations. In this model there is symmetry
 in luminance about the zenith direction. The zenith lumi-
 nance is three times greater than the luminance near the
 horizon. For the clear-sky model the formulation of *Kittler*
 [1967], which was subsequently adopted by the International
 Commission on Illumination [*Commission Internationale*
de l’Eclairage, 1973], was used. The model is not for a pure
 Rayleigh sky, but includes realistic aerosol scattering that

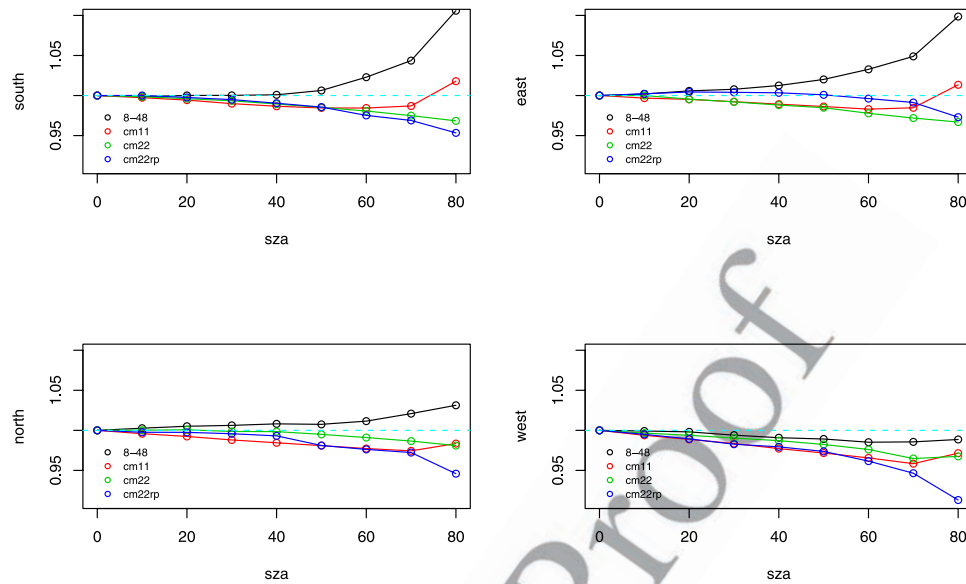


Figure 6. Angular responses in four cardinal directions (signal cable north) for the four pyranometers in the IOP.

379 produces circumsolar brightening and enhanced luminance
380 near the horizon.

381 [24] The calculations were performed for pyranometers
382 calibrated at a solar zenith angle of 45° and placed on
383 trackers that always orient the pyranometers in the same
384 direction relative to the Sun as in this study. Corrections for
385 these two skies and these four pyranometers were per-
386 formed. Table 3 contains the required correction factors
387 for skylight with the Sun at 45° using the cosine responses
388 from Figure 6. For example, the 8–48 for a cloudy sky
389 (Moon-Spencer) has to be divided by 1.0004, while the
390 cm22 has to be divided by 0.9999, to correct for the
391 deviations from a true cosine response. For a clear sky
392 (CIE-Clear) the correction for the 8–48 is division by
393 1.0044 and the correction for the cm22rp is division by
394 0.9949. By comparing the ratio of 1.0004/0.9999 in cloudy
395 skies to 1.0044/0.9949 in clear skies, the 8–48 shows a
396 relative shift of 0.9% up with respect to the cm22rp as the
397 sky changes from cloudy to clear. Through the same
398 reasoning the cm11 shifts up by 0.3% relative to the cm22rp
399 from cloudy to clear skies, and the cm22 shifts up by 0.4%.
400 The corrections for the Sun at 30° elevation are about half
401 that at 45° .

402 [25] The spectral and angular response effects, combined,
403 result in a 0.4% shift up in changing from cloudy to clear for
404 the cm22 relative to the cm22rp. The combined effects for
405 the cm11 relative to the cm22rp yield a net shift down by
406 about 0.9% from cloudy to clear since the spectral shift
407 down is partially canceled by the angular response shift up.
408 The 8–48 spectral and angular shifts in changing from
409 cloudy to clear conditions are in the same direction relative
410 to the cm22rp and are 2.4% up. Examination of Figure 4
411 qualitatively agrees with these calculations. There is fair
412 quantitative agreement in shifts for the cm11 and cm22
413 relative to the cm22rp. The 8–48, indeed, reads higher than
414 the cm22rp when it is clear, but only about half of the

increase (2.4% versus 5.2%) is explained by the spectral and
angular corrections. 415 416

5. Other Measurements of Diffuse Compared to IOP Pyranometers 417 418

[26] Two 8–48 pyranometers are included as part of the
permanent instrument array at the ARM SGP site. These
SGP 8–48s are separated by about 450 m from the radiation
calibration facility (RCF) where the IOP measurements
were made. Cloudy skies produce noisier comparisons
because of the distance separation than clear skies. On
average these two station 8–48s compared to the cm22rp
are 5.3% and 3.1% higher when it is clear than when it is
cloudy. The differences among the three 8–48s suggest that
the spectral and cosine effects differ among instruments.
Whether the differences are primarily angular or spectral for
a particular instrument is impossible to assign without
detailed characterizations. Calibration of the pyranometer
at a solar-zenith angle of 45° minimizes the effects of
angular response on the diffuse irradiance for all pyranom-
eters with angular responses similar to those measured. This
can be qualitatively understood because the diffuse signal is
nearly proportional to $\sin(\theta) \bullet \cos(\theta) = \sin(2\theta)/2$, which
peaks at 45° . For this reason most of the difference can be
attributed to the spectral response of the 8–48. In the
current IOP the actual reflection from the black and white
sectors was not measured, but coupons made of the same
substrates coated in a similar way to the sectors of the 8–48

Table 3. Corrections (Divisors) to Diffuse for Imperfect Angular Response for Sun at 45° t3.1

Model Sky	cm22rp	8–48	cm11	cm22	t3.2
Moon-Spencer	0.9999	1.0004	1.0030	0.9920	t3.3
CIE-Clear	0.9949	1.0044	1.0012	0.9912	t3.4

t4.1 **Table 4.** Integrated RSS Data Plus Added Modeled Spectra Compared to Measured Diffuse/Direct

t4.2	Date 2006	LT	Measured Direct	Diffuse cmxx/8-48	RSS+ Diffuse	SMARTS Direct	SMARTS Diffuse
t4.3	11 Oct	0900	874.8 nip	54.4/56.7	53.0	871.3	60.3
t4.4	11 Oct	1100	962.5 cav.	64.7/67.4	64.7	957.8	69.2
t4.5	12 Oct	1433	914.8 nip	66.6/68.8	65.1	909.7	69.0
t4.6	13 Oct	1200	897.1 cav.	100.7/105.9	100.4	902.4	102.0

442 were used as proxies for the actual reflectivities. Coupon
 443 differences from the actual 8–48 surfaces may account for
 444 why only about one half of the increase could be explained.
 445 [27] An entirely different measurement of diffuse that
 446 may help point to the true diffuse irradiance is the spectral
 447 diffuse irradiance measurement of the rotating shadowband
 448 spectroradiometer (RSS) [Harrison *et al.*, 1999]. The
 449 RSS data using a Langley-plot calibration technique to
 450 determine spectral sensitivity [Kiedron *et al.*, 2002] give
 451 an integrated diffuse value at 1433 local time (LT) on 12
 452 October 2006 that totals 54.8 W/m² between 361.5 and
 453 1074 nm. The corresponding uncertainty in integrated RSS
 454 diffuse measurement is estimated at about 3%. To estimate
 455 the unmeasured spectral irradiance we used the SMARTS
 456 radiative transfer model [Gueymard, 2001] with inputs of
 457 measured aerosol properties (column aerosol optical depth
 458 at five wavelengths, ground-level measurements of aerosol
 459 properties to estimate single scattering albedo and asymmetry
 460 parameter), water vapor column, ozone column, and esti-
 461 mated spectral surface albedos. Integrating model output
 462 between 280 and 361.5 nm yields 8.2 W/m² and between
 463 1074 and 4000 nm another 2.1 W/m² for a total of 65.1 W/
 464 m². The measured diffuse for that same time for the cm11 is
 465 66.4 W/m²; for the cm22 is 66.9 W/m²; for the cm22rp is
 466 66.6 W/m²; and for the 8–48 is 68.8 W/m². The RSS
 467 measured diffuse was added to the model runs (designated
 468 RSS+) on three other occasions for the total of four cases
 469 that are summarized in Table 4. All four skies were
 470 cloudless. The measured direct with the Eppley NIP or
 471 the Eppley HF cavity radiometer are given in the third
 472 column to be compared with the SMARTS model results in
 473 the sixth column. All direct results show excellent agree-
 474 ment to within about 5 W/m². The fourth column lists two
 475 measured diffuse values; the first is the average of three
 476 cmxx instruments, which are within 0.6 W/m² of each other
 477 in all four cases, and the second entry is the 8–48 reading.
 478 The summed spectral diffuse in column five is closer to the
 479 average of three cmxx pyranometers with the largest differ-
 480 ence 1.5 W/m². The difference between the summed spec-
 481 tral diffuse and the 8–48 varies between 2.7 and 5.5 W/m².
 482 Note that the summed SMARTS modeled spectral diffuse
 483 between 280 and 4000 nm is higher than the measurement
 484 for low aerosol cases, but agrees rather well for the higher
 485 aerosol case on 13 October.

486 [28] A point that can be made is that all Kipp and Zonen
 487 instruments are constructed similarly, and, therefore, would
 488 be expected to agree. Of course, each cmxx instrument in
 489 this study is different in some detail; the cm11 has a
 490 different glass dome than the cm22s, and cm22rp has a
 491 heater and a different ventilator than the cm22. An instru-
 492 ment that is different than the Kipp and Zonen pyranometers
 493 and different than the Eppley 8–48 is the Eppley PSP. The
 494 ventilated Eppley PSP has one of the largest offsets known

for a ventilated pyranometer [see, e.g., Michalsky *et al.*, 495
 2003, Figure 10]. Philippona [2002], however, demonstrated 496
 that with proper heating and ventilation of the PSP this 497
 offset could be eliminated. A PSP that was shade/unshade 498
 calibrated at NREL was operated in the same type of 499
 ventilator as in the Philippona [2002] study in a follow-on 500
 experiment to the October 2006 IOP. This instrument/ 501
 ventilator combination was colocated in Boulder, Colorado, 502
 with the cm22 and the 8–48 used in the earlier IOP. Figure 503
 7 is a plot of diffuse irradiance from two clear days as 504
 identified by the direct irradiance, scaled and overplotted in 505
 gray. The offset for the PSP, while noisy, oscillates about 506
 zero irradiance. An analysis of the nighttime data for eight 507
 nights for the PSP yields a probability distribution that is 508
 symmetric and peaks at zero irradiance. From Figure 7 it is 509
 clear that the PSP agrees better with the cm22 than the 8– 510
 48. Although not conclusive, since this PSP’s angular and 511
 spectral responses were not measured, this lends additional 512
 support to the proposition that cmxx instruments are making 513
 better diffuse measurements than the 8–48. 514

6. Summary 515

[29] Reda *et al.* [2003] have estimated the uncertainty of 516
 diffuse irradiance measurements made with Eppley 8–48s. 517
 They concluded that the Eppley 8–48 could be used to 518
 measure diffuse with an uncertainty of $\pm(3\%$ of reading + 519
 1 W/m²). The current study suggests that there is agreement 520
 at least at this level or even better when overcast conditions 521
 prevail among all four pyranometers. However, when the 522
 sky is clear, five of six 8–48s have a high bias, which 523
 ranges between 2–5%, with respect to the other three 524
 measurements of diffuse irradiance in the IOP. Comparisons 525
 during the IOP suggest that the cm22rp and cm22 are 526
 usually in agreement at the 0.5% level, or better, for cloudy 527
 or clear conditions. When either of these instruments is 528
 compared to the 8–48 in the IOP, the results range between 529
 agreeing when it is cloudy to over 5% disparity when it is 530
 clear, with the 8–48 higher. Repeating this comparison 531
 (cloudy ratio of pyranometers to clear ratio) using the two 532
 permanent central facility 8–48s at the ACRF during the 533
 IOP resulted in 8–48s reading higher by 3.1% and 5.3% 534
 relative to the trio of Kipp and Zonen pyranometers in this 535
 IOP. A follow-on study comparing three Boulder station 8– 536
 48s with the cm22 from the IOP produced 8–48/cm22 537
 ratios between cloudy and clear skies that were –0.2%, 538
 1.9%, and 3.9% for three pyranometers. This expands the 539
 range of variability that is seen among 8–48 responses and 540
 further weakens the case for their use in establishing a 541
 diffuse irradiance standard. 542

[30] Integrated RSS spectral irradiance measurements 543
 over most of the clear diffuse spectrum that were calibrated 544
 by the Langley method were made and then augmented with 545

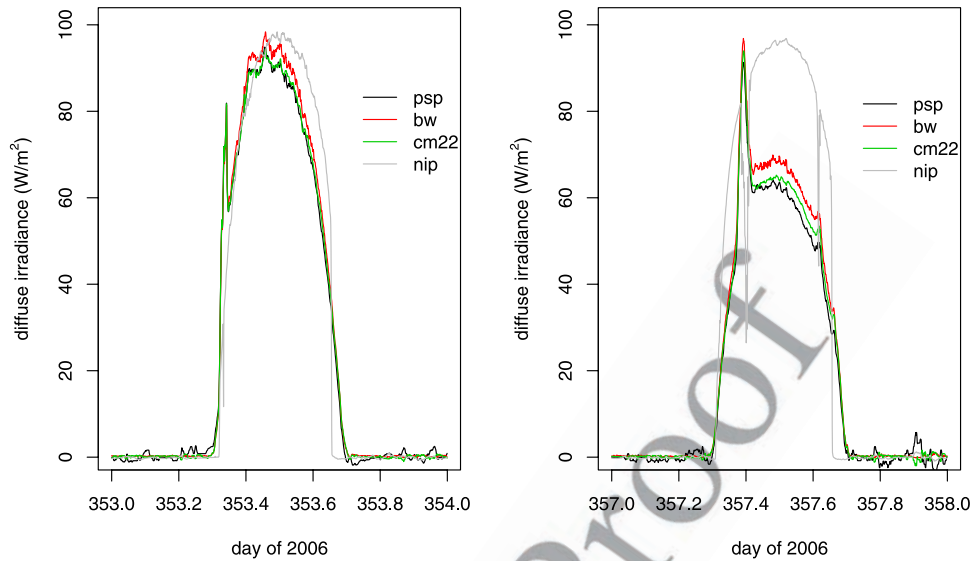


Figure 7. Diffuse irradiance from two clear days in Boulder, Colorado, in 2006 with two pyranometers from this IOP and a PSP operated in a *Philipona* [2002]–style ventilator and heater system that eliminates zero offsets. The scaled direct irradiance is in gray to confirm the clarity of the atmosphere. The diffuse measured by the cm22 and the PSP are in close agreement.

546 a model for the missing $\approx 15\%$ of the irradiance not
 547 measured. The additional modeled irradiance should affect
 548 the integrated spectral irradiance uncertainty by no more
 549 than 1 W/m^2 . The four cases studied suggested closer
 550 agreement with the cmxx instruments than with the 8–48.
 551 This independent result supports the proposition that the
 552 cmxx trio makes a more accurate diffuse measurement.
 553 [31] A different instrument, the PSP by the same manu-
 554 facturer of the Eppley 8–48, was operated in a heated
 555 ventilator that eliminated its typically large offset. Although
 556 not corrected for angular and spectral responses, this shade/
 557 unshade calibrated PSP agreed better with the cmxx trio
 558 than the 8–48 in side-by-side measurements providing
 559 additional support for the cmxx standard.

560 7. Conclusions

561 [32] Using the cm11, cm22, and cm22rp average as the
 562 standard for diffuse irradiance, an uncertainty at the 95%
 563 confidence level is estimated at $\pm(2.2\%$ of reading + 0.2 W/
 564 $\text{m}^2)$. That this is a reasonable estimate is illustrated in the
 565 bottom of Figures 4 and 5 where the departures from unity
 566 among the ratios are within the bounds of the $\pm 2\%$ lines. For
 567 this uncertainty determination guidance provided by Cook
 568 [1999] was used. The statistical component of the uncertainty
 569 (Type A uncertainty) came from adding, in quadrature, the
 570 95% cavity uncertainty (0.45%) and twice the standard
 571 deviation of the mean (0.10%) from the 30 measurements
 572 used to obtain calibration constants from the shade/unshade
 573 calibration sequence. The largest uncertainties are of the
 574 B type (those not based on a statistical calculation). These
 575 came predominantly from the angular responses, the spectral
 576 responses, and the temperature dependences. The largest
 577 deviations from the “perfect” response as modeled in Table 2
 578 for spectral response (1.2%) and Table 3 for angular
 579 response (0.88%), and for temperature response (1.0%)
 580 based on manufacturer specifications were used as the

half-widths of rectangular distributions. Other type B errors, 581
 for example, the resolution of the data acquisition system, 582
 were found to be much smaller and negligible relative to 583
 these. The three standard uncertainties were added in 584
 quadrature to obtain the type B uncertainty estimate. This 585
 type B uncertainty was doubled and squared and added to 586
 the type A uncertainty (as given above) squared. The square 587
 root is the 2.2% stated uncertainty. The added 0.2 W/m^2 588
 reflects the estimated ability to correct the zero offset for 589
 these three instruments. 590

[33] Similar results should be possible by following the 591
 steps outlined in this paper. Specifically, it is assumed that 592
 one uses shaded and ventilated pyranometers and a shaded 593
 and ventilated pyrgeometer. The pyrgeometer is used to 594
 derive a nighttime relationship between pyranometer offset 595
 and pyrgeometer reading that is used to correct all pyran- 596
 ometer offsets, day or night. Further, this assumes that the 597
 pyranometers are calibrated using a shade/unshade method 598
 as outlined in this paper with simultaneous measurements of 599
 direct beam irradiance using an absolute cavity radiometer 600
 with the Sun within $1\text{--}2^\circ$ of 45° solar-zenith angle. Note 601
 that the shading of the pyranometers uses tracking shading 602
 disks, not fixed shadowbands, which would block much 603
 more of the sky than the area around the solar disk. Some 604
 assurance that the angular response is no worse than the 605
 instruments in this paper, based on measurements provided 606
 by the manufacturer or made in one’s own laboratory, 607
 should be obtained. The requirement for data acquisition 608
 with a resolution of 0.05 W/m^2 can usually be met with 609
 modern field data loggers. 610

[34] This approach should minimize the uncertainty in 611
 diffuse irradiance measurements, if side-by-side calibrations 612
 of shaded pyranometers using the cmxx trio cannot be 613
 made. 614

[35] **Acknowledgments.** The authors thank Afshin Andreas for 615
 programming the data loggers and performing the data collection during 616

617 the IOP. Craig Webb helped set up the experiment at the ARM ACRF
 618 in Oklahoma. Ihab Abboud measured the angular responses of four
 619 pyranometers. Chris Cornwall helped in setup and data collection for the
 620 Boulder measurements. Robert Dolce of Kipp & Zonen, Inc. and Tom Kirk
 621 of Eppley Laboratory, Inc., provided information on the spectral properties
 622 of the absorbing surfaces and the transmission of the pyranometer domes.
 623 The reviewers provided comments that led to notable improvements in this
 624 paper. This work was performed in collaboration with the U.S. Department
 625 of Energy through its support of the Atmospheric Radiation Measurement
 626 Program Climate Research Facility.

627 References

628 Commission Internationale de l'Eclairage (1973), Standardization of Lumi-
 629 nance Distribution on Clear Skies, *CIE Publ.*, 22, Paris.
 630 Cook, R. R. (1999), Assessment of uncertainties of measurement for cali-
 631 bration and testing laboratories, 57 pp., Natl. Assoc. of Test. Auth., N. S.
 632 W., Silverwater, Australia.
 633 Dutton, E. G., J. J. Michalsky, T. Stoffel, B. W. Forgan, J. Hickey, D. W.
 634 Nelson, T. L. Alberta, and I. Reda (2001), Measurement of broadband
 635 diffuse solar irradiance using current commercial instrumentation with a
 636 correction for thermal offset errors, *J. Atmos. Oceanic Technol.*, 18, 297–
 637 314.
 638 Gueymard, C. A. (2001), Parameterized transmittance model for direct
 639 beam and circumsolar spectral irradiance, *Sol. Energy*, 71, 325–346.
 640 Harrison, L., M. Beauharnois, J. Berndt, P. Kiedron, J. Michalsky, and Q. L.
 641 Min (1999), The rotating shadowband spectroradiometer (RSS) at SGP,
 642 *Geophys. Res. Lett.*, 26, 1715–1718.
 643 Kiedron, P. W., L. Harrison, J. J. Michalsky Jr., J. A. Schlemmer, and J. L.
 644 Berndt (2002), Data and signal processing of rotating shadowband spec-
 645 troradiometer (RSS) data, *Proc. SPIE Int. Soc. Opt. Eng.*, 4815, 58–72.
 646 Kittler, R. (1967), Standardization of outdoor conditions for the calculation
 647 of daylight factor with clear skies, paper presented at CIE International
 648 Conference on Sunlight in Buildings, Int. Comm. on Illumination, Bouw-
 649 centrum, Amsterdam.

Michalsky, J. J., et al. (2003), Results from the first ARM diffuse horizontal
 shortwave irradiance comparison, *J. Geophys. Res.*, 108(D3), 4108,
 doi:10.1029/2002JD002825. 650
 651
 652
 Michalsky, J. J., et al. (2005), Toward the development of a diffuse hor-
 izontal shortwave irradiance working standard, *J. Geophys. Res.*, 110,
 D06107, doi:10.1029/2004JD005265. 653
 654
 655
 Michalsky, J. J., G. P. Anderson, J. Barnard, J. Delamere, C. Gueymard,
 S. Kato, P. Kiedron, A. McComiskey, and P. Ricchiazzi (2006), Short-
 wave radiative closure studies for clear skies during the Atmospheric
 Radiation Measurement 2003 Aerosol Intensive Observation Period,
J. Geophys. Res., 111, D14S90, doi:10.1029/2005JD006341. 656
 657
 658
 Moon, P., and D. Spencer (1942), Illumination from a non-uniform sky,
Illuminating Eng., 37, 707–726. 659
 660
 661
 Philipona, R. (2002), Underestimation of solar global and diffuse radiation
 measured at Earth's surface, *J. Geophys. Res.*, 107(D22), 4654,
 doi:10.1029/2002JD002396. 662
 663
 664
 Reda, I., T. Stoffel, and D. Myers (2003), A method to calibrate a solar
 pyranometer for measuring reference diffuse irradiance, *Sol. Energy*, 74,
 103–112. 665
 666
 667
 668
 669
 670
 671
 672
 673
 674
 675
 676
 677
 678
 679
 680
 681
 C. Gueymard, Solar Consulting Services, P.O. Box 392, Colebrook, NH
 03576, USA.
 P. Kiedron, Cooperative Institute for Research in Environmental
 Sciences, University of Colorado, Boulder, CO 80309, USA.
 L. J. B. McArthur, Meteorological Service of Canada, Downsview, ON,
 Canada M3H 5T4.
 J. J. Michalsky, Earth System Research Laboratory, NOAA, Boulder, CO
 80305, USA. (joseph.michalsky@noaa.gov)
 R. Philipona, Physikalisch-Meteorologisches Observatorium Davos,
 World Radiation Center, CH-7260 Davos, Switzerland.
 T. Stoffel, National Renewable Energy Laboratory, Golden, CO 80401,
 USA.